


Research Article

Cyanidin-3-O-Glucoside Combined with PGC1 α Inhibitor Promotes Cancer Cell Death by Inducing Excessive Levels of ROS in Cervical Squamous Cell Carcinoma

Lili Liu,^{1,2} Tao Zhao,³ Huaping Yang,³ Zhenghui Hu,³ and Caifeng Xie ³

¹Department of Pharmacy, The First Affiliated Hospital of Nanchang University, Jiangxi Medical College, Nanchang University, Nanchang, Jiangxi, China

²School of Pharmacy, Jiangxi Medical College, Nanchang University, Nanchang, Jiangxi, China

³School of Basic Medical Sciences, Jiangxi Medical College, Nanchang University, Nanchang, Jiangxi, China

Correspondence should be addressed to Caifeng Xie; xiECAIFENG@ncu.edu.cn

Received 10 October 2023; Revised 26 January 2024; Accepted 30 January 2024; Published 16 February 2024

Academic Editor: Akhilesh K. Verma

Copyright © 2024 Lili Liu et al. This is an open access article distributed under the Creative Commons Attribution License, which permits unrestricted use, distribution, and reproduction in any medium, provided the original work is properly cited.

Cervical cancer is a global public health problem, particularly in the low-income and middle-income countries. Natural products, such as cyanidin and its derivative cyanidin-3-O-glucoside (C3G), are considered safe and nontoxic food additives, potent therapeutic options for cancer. The present study aims to evaluate the beneficial effects of C3G on cervical squamous cell carcinoma (CSCC) *in vitro* and explore more potential therapeutic strategies for CSCC. C3G significantly inhibited the cell growth of CSCC cells and induced cancer cell apoptosis in a dose-dependent manner. Meanwhile, C3G promoted cellular reactive oxygen species (ROS) accumulation and decreased mitochondrial membrane potential and mitochondrial mass. The antioxidant agent N-acetyl-L-cysteine (NAC) rescued the effect of C3G on CSCC cells, further demonstrating ROS's important role in C3G treatment. To explore the underlying mechanism, autophagy-related signaling pathways were investigated, and the results showed that C3G induced cell autophagy but not mitophagy. More importantly, C3G caused a significant activation of mitochondria biogenesis through the peroxisome proliferator-activated receptor gamma coactivator 1 alpha (PGC-1 α) signaling pathway. C3G synergized with PGC-1 α inhibitor SR-18292 induced more severe ROS accumulation and showed more potent inhibition of cell proliferation and mitochondrial membrane potential than C3G treatment alone. Thus, the present study suggests a new potential therapeutic strategy for CSCC based on the synergistic effect of C3G and PGC1 α inhibitors.

1. Introduction

Globally, cervical cancer ranks as the fourth most frequently diagnosed cancer and the fourth leading cause of cancer death in women, which represents a major worldwide health challenge [1]. The most common histological subtypes of cervical cancer are squamous cell carcinoma (70%) and adenocarcinoma (25%). Persistent infection with a high-risk subtype of human papillomavirus (HPV-16 and HPV-18) is considered the primary cause of cervical cancer [2, 3]. Cervical cancer is a largely preventable disease with adequate screening and HPV vaccination. However, for those patients who have been at later stages of cervical cancer or come from low-income

and middle-income countries, the treatment of cervical cancer is still a big problem [4, 5]. Besides the standard treatment by concurrent radiation plus cisplatin (CDDP)-based chemotherapy, many other therapeutic strategies, including bioactive compounds derived from natural products, have been developed in recent years [6–8].

Reactive oxygen species (ROS) are generally defined as a group of highly reactive molecules that play critical roles in the pathogenesis of various human diseases, including cancer [9]. It is now well accepted that the production of ROS is elevated in tumor cells because of the increased metabolic rate, gene mutation, and relative hypoxia [10]. Although increased ROS concentrations play crucial roles in cancer formation and progression, levels above

a cytotoxic threshold cause cancer cell death by triggering programmed cell death (PCD) or senescence [11]. Therefore, anticancer therapies based on oxidative damage through the acceleration of accumulative ROS or the defective antioxidant system in cancer cells have been developed [12, 13]. Many chemotherapeutics induce oxidative stress and ROS-mediated cell damage in cancer cells by increasing ROS above the threshold to yield an anticancer effect [14]. The transcriptional coactivator peroxisome proliferator-activated receptor γ coactivator-1 α (PGC-1 α) is considered as a master regulator of mitochondrial lifecycle and ROS stress response [15]. The internal accumulation of ROS in the cytosol and mitochondria usually causes damage to cells. Under such conditions, PGC1 α is required for antioxidant defense by inducing the expression of ROS-detoxifying proteins, such as GPx1 and SOD2 [16].

Cyanidin-3-O-glucoside (C3G) is one of the most common anthocyanins in vegetables and fruits, especially edible berries [17, 18]. It has been reported that C3G exerts potential antitumor effects in various types of cancers by modifying the redox state and regulating the basic physiological activities of cells [19–21]. Some previous studies indicated that C3G had an antioxidant effect on cancer cells [22, 23]. In contrast, others challenged this conclusion and pointed out that C3G may increase cancer cells' intracellular reactive oxygen species (ROS) levels [24, 25]. In addition, some studies further indicated that the anticarcinogenic efficiency of C3G is lower than cyanidin due to the existence of a sugar group [26]. To clarify the exact role of C3G on ROS accumulation in cancer and explore the underlying molecular mechanism, we investigate the ROS regulatory effect of C3G in cervical squamous cell carcinoma (CSCC) in the present study.

Currently, the effect of C3G on cervical cancer is largely unknown. Studies have demonstrated that C3G combined with cisplatin can inhibit cell proliferation and induce oxidative stress, meanwhile downregulating the PI3K/AKT/mTOR or Nrf2 pathway in the cervical adenocarcinoma HeLa cells [24, 27]. However, whether C3G possesses the same effect on cervical squamous cell carcinoma is unknown, and the mechanisms underlying the ROS accumulation in cancer cells by C3G are still unclear. Further, how to improve the therapeutic efficiency of C3G also needs to be addressed. The present study explores a new therapeutic strategy for CSCC by C3G based on its oxidative stress-inducing activity and determines the underlying mechanism.

2. Materials and Methods

2.1. Cell Culture. Human cervical squamous cell carcinoma (CSCC) cell lines SiHa and HCC94 were obtained and cultured as previously described [28]. Among them, SiHa is a cell line isolated from fragments of a primary uterine tissue sample from a 55-year-old, female, Japanese patient with squamous cell carcinoma. HCC94 is a cell line established from cervix uteri tissue sample from a 37-year-old, female, Chinese patient with squamous cell carcinoma [29]. Briefly,

SiHa cells were cultured in Dulbecco's modified Eagle's medium (DMEM) supplemented with 10% fetal bovine serum (FBS, Invitrogen, CA, USA), and HCC94 cells were cultured in the RPMI-1640 medium containing 10% FBS. All cells were incubated in a humidified incubator with 5% CO₂ at 37°C.

2.2. Cell Growth Assay. SiHa and HCC94 cells were seeded at a density of 1×10^4 cells in 24-well plates. Cultured overnight, cells were treated with different concentrations of C3G (0, 4, 8, 12, 16, 20 μ M, dissolved in DMSO) for 48 hours. C3G (purity > 98%, HPLC) was purchased from Meilune Biotechnology Co., Ltd (Dalian, China). After treatment, cell images were obtained and fixed with 4% formaldehyde for 30 min. Finally, cells were stained with 0.1% crystal violet, and the cell number was calculated.

2.3. EdU (5-Ethynyl-2'-deoxyuridine)/Hoechst 33342 Staining Assay. SiHa and HCC94 cells were seeded at a density of 2×10^4 cells in 24-well plates and treated with DMSO, C3G alone (8 μ M), NAC alone (10 μ M), and C3G (8 μ M) combined with NAC, PGC1 α inhibitor SR18292 alone (), and C3G (8 μ M) combined with SR18292 (10 μ M) for 48 hours, respectively. Cells were stained, and the newly synthesized DNA of the cells was evaluated by the EdU incorporation assays using a Cell Proliferation EdU Image Kit (Green Fluorescence) (Cat No: KTA2030, Abbkine, Inc, USA) according to the manufacturer's instructions. The labeled DNA in the cells was analyzed by using a fluorescence microscope (Ex/Em: 501/525 nm), and the nucleus was detected by Ex/Em: 360/460 nm. Images of the EdU positive cells (red cells) and total Hoechst33342 positive cells (blue cells) were obtained using a fluorescence microscope and calculated using Image Pro Plus 6.0.

2.4. Flow Cytometry. SiHa and HCC94 cells were treated with different concentrations of C3G (0, 4, 8, 12, 16, 20 μ M, dissolved in DMSO) for 48 hours and then collected for staining. Cells were stained with 5 μ L Annexin V-FITC and 10 μ L PI Staining Solution by using an Annexin V-FITC Apoptosis Detection Kit (No. C1062M, Beyotime Biotechnology Co., Ltd, Shanghai) according to the manufacturer's instructions. Then, stained cells were subject to FACS analysis in one hour. Annexin V-FITC was detected at Ex/Em: 488/525 nm using a FITC signal detector (FL1), and PI-DNA complex was detected at Ex/Em: 535/615 nm (FL3). The percentage of Annexin V-positive cells was calculated and analyzed using FlowJo software (Tree Star, USA).

2.5. ROS Level Detection. Intracellular reactive oxygen species (ROS) levels were measured using the fluorescent dye DCFH-DA. Briefly, SiHa and HCC94 cells were treated with different concentrations of C3G or other reagents for 48 hours, and then cells were collected and stained by DCFH-DA. Cells were washed three times after staining, and

the fluorescence intensity was detected. ROS accumulation of each group was normalized to the control group (DMSO solution treatment). N-Acetyl-L-cysteine (NAC) was used as an antioxidant reagent for the ROS rescue experiment. HCC94 cells were treated with DMSO, C3G alone (8 μ M), NAC alone (10 μ M), and C3G combined with NAC for 48 h, respectively. Then, cell images were obtained using the microscope.

2.6. JC-1 Mitochondrial Membrane Potential Assay. Mitochondrial membrane potential was determined by JC-1 fluorescent staining. HCC94 cells were cultured in 6-well plates and treated with different concentrations of C3G (0, 8, 20 μ M, dissolved in DMSO) or the combination of C3G (8 μ M) and NAC (or PGC1 α inhibitor SR18292) for 48 hours. After treatment, cells were washed with PBS and stained with JC-1 working solution for 20 minutes at 37°C. Cells were washed with washing buffer and imaged using a fluorescence microscope.

2.7. MitoTracker Green Staining. The mitochondrial mass of the cell was monitored by using the probe MitoTracker Green since this reagent labels mitochondria in a manner that is independent of the membrane potential. HCC94 cells were cultured in 6-well plates and treated with different concentrations of C3G (0, 8, 20 μ M, dissolved in DMSO) for 48 hours. After treatment, the culture medium was discarded, and cells were stained using a Mito-Tracker Green staining solution (No. C1048, Beyotime Biotechnology Co., Ltd, Shanghai) for 20 minutes at 37°C. After staining, the fresh culture medium was added to the wells, and images were obtained using a fluorescence microscope.

2.8. Western Blotting. SiHa and HCC94 cells were treated with different concentrations of C3G or the combination with NAC and PGC1 α inhibitor SR18292 for 48 hours. After treatment, cells were washed with a cold PBS buffer and collected. Then, cells were lysed, and total proteins were extracted. The specific protein levels in the samples were determined by the Western blot assay as previously described [30]. Briefly, proteins were separated on SDS-PAGE gel and transferred to PVDF membranes and then blocked with 5% BSA. Then, PVDF membranes were incubated with the indicated primary and secondary antibodies. A prolight chemiluminescence detection kit was used to visualize protein bands, and images were taken by a digital gel image analysis system. The relative protein levels were analyzed by densitometry using ImageJ software. Furthermore, the primary antibodies were listed in Table S1.

2.9. Statistical Analysis. The GraphPad Prism software (Version 9.0.0, GraphPad Software Inc., San Diego, CA, USA) for Windows was used to analyze the data. The data were shown as the mean \pm S.E.M. Differences between the groups were calculated by ANOVA or Student's *t*-test where appropriate. **P* < 0.05 was considered significant.

3. Results

3.1. C3G Inhibited Cell Growth of Human CSCC. The effect of cyanidin-3-O-glucoside (C3G, Figure 1(a)) on human cervical squamous cell carcinoma (CSCC) cell lines HCC94 and SiHa was determined. Cancer cells were treated with a series of concentrations of C3G, and the cell number was calculated after 48 hours of treatment. The results demonstrated that C3G significantly suppressed the cell growth of both HCC94 and SiHa with more significant inhibition of the HCC94 cell (Figures 1(b) and 1(c)). Cell viability was dramatically decreased from the concentration of 4 μ M and 8 μ M of C3G in HCC94 and SiHa, respectively. Furthermore, representative images of HCC94 cells treated with various concentrations of C3G were obtained, showing that C3G inhibited cell growth and the cells are likely to undergo cell apoptosis or death (Figure 1(d)).

3.2. C3G Promoted Cell Apoptosis of CSCC Cells. Because C3G suppressed the cell growth of CSCC cells, we further investigated whether the cell growth inhibition was partially affected by the alteration of cell apoptosis. The cell apoptosis was detected by the flow cytometry assay using Annexin V/PI staining, and the percentage of Annexin V-positive cells was calculated and analyzed. The results showed that C3G treatment induced a modest cell apoptosis of HCC94 (Figure 2(a)) and SiHa cells (Figure 2(b)) at 8 μ M and a significant cell death at the concentration above 12 μ M.

3.3. C3G Increased the Accumulation of ROS in CSCC Cells. Excess cellular levels of reactive oxygen species (ROS) and mitochondrial dysfunction would lead to the activation of cell apoptosis [10, 31]. Therefore, we first investigated the level of ROS in CSCC cells with C3G treatment. The results showed that the levels of cellular ROS in both HCC94 (Figure 3(a)) and SiHa (Figure 3(b)) cells were elevated in a modestly dose-dependent manner, which indicated that C3G would accelerate the accumulation of cellular ROS in CSCC cells. Furthermore, the ROS rescue experiment was performed to confirm the effect of C3G on the CSCC cells. As shown in Figure 3(c), HCC94 cells treated with C3G (8 μ M) undergo a cell death process while being rescued by coculturing with the antioxidant reagent N-acetyl-L-cysteine (NAC).

3.4. C3G Caused Mitochondrial Dysfunction of CSCC Cells. Mitochondrial dysfunction is suggested to have initiated cell apoptosis and may play a central role in the apoptotic pathway [32, 33]. Meanwhile, mitochondrial membrane potential ($\Delta\psi_m$) regulates mitochondrial homeostasis by selective elimination of dysfunctional mitochondria, and the reduction of mitochondrial membrane potential is considered to be a hallmark of mitochondrial dysfunction [34, 35]. Therefore, we further detected the effect of C3G on the mitochondrial membrane potential alteration in CSCC cells (Figure 4(a)). The results showed that C3G treatment decreased the fluorescence intensity of the JC-1 aggregate

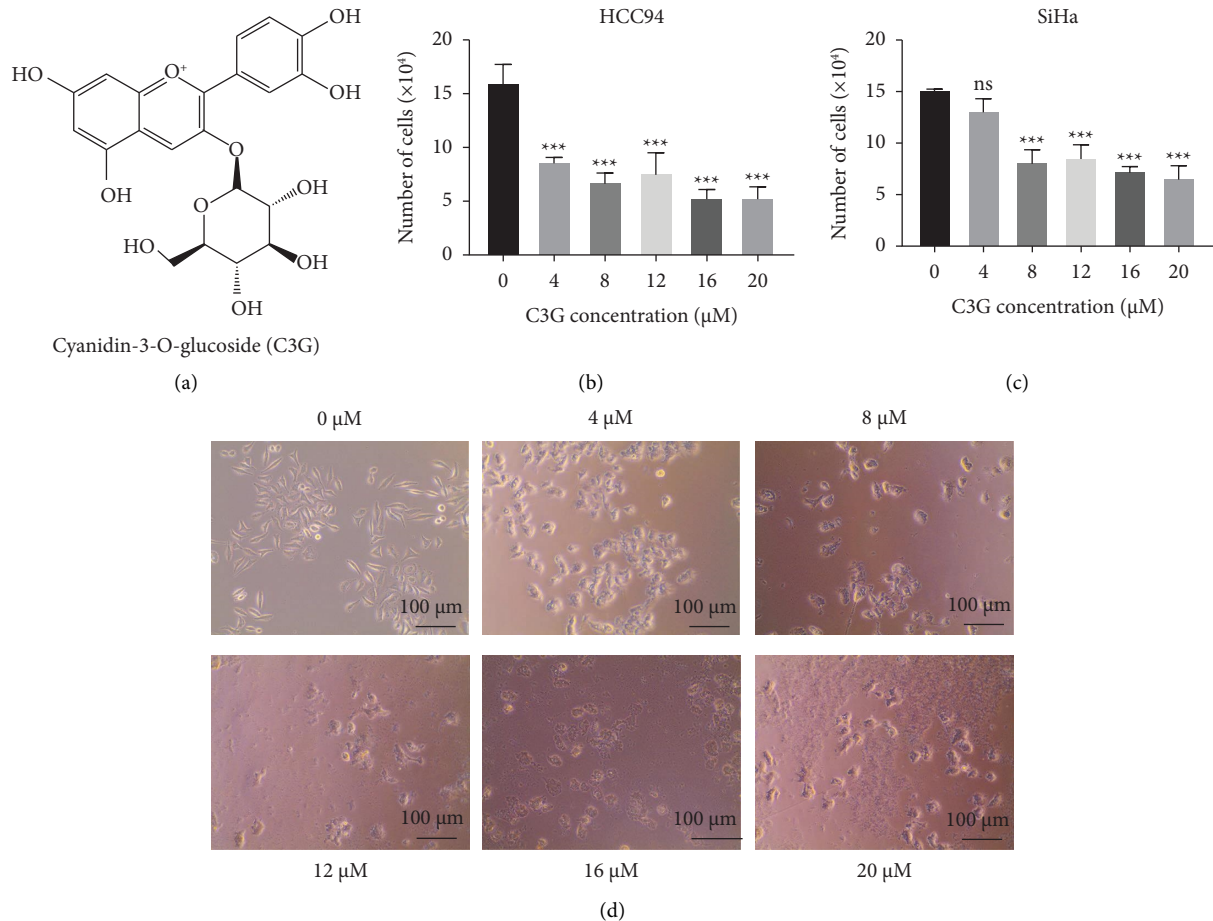


FIGURE 1: (a) The chemical structure of cyanidin-3-O-glucoside (C3G) by ChemDraw 17.0; (b, c) Cell growth of HCC94 and SiHa with different concentrations of C3G (0, 4, 8, 12, 16, 20 μM) for 48 h. (d) HCC94 cell images were obtained by using a microscope after being treated with C3G (0, 4, 8, 12, 16, 20 μM) for 48 h (magnification: 100x). Data are expressed as the mean \pm S.E.M. *** P < 0.001, ns: nonsignificant differences. The scale bar is 100 μm .

(Red), indicating the reduction of the mitochondrial membrane potential at different concentrations. It showed more potential on the $\Delta\psi\text{m}$ reduction at 8 μM than 20 μM . To further assess the mitochondrial mass of HCC94 treated with C3G, the Mito-track green staining assay was performed (Figure 4(b)). The results indicated that C3G decreased the mitochondrial mass at 8 μM while partially recovering it at 20 μM , which somehow further confirmed the conclusion derived from the mitochondrial membrane potential assay.

3.5. C3G Promoted Mitochondrial Biogenesis of CSCC Cells and Accelerated the Accumulation of ROS Combined with PGC1 α Inhibitor. As shown by the results of Mito-track green staining, mitochondrial mass was increased at the high-concentration treatment of C3G (20 μM) compared to that at medium concentration treatment (8 μM). The mechanism underlying this phenomenon would be activating the self-repairing system of mitochondria through autophagy or mitophagy [36, 37]. Therefore, we investigated the effect of C3G on the signaling pathways involved in

CSCC cell autophagy and mitophagy using Western blot. As shown in Figure 5(a), C3G significantly induced the cleaved microtubule-associated protein 1 A/1B-light chain 3 (LC3) protein, a valuable indicator of autophagosome initiation [38]. At the same time, the upstream signaling pathway was also activated, as indicated by the decreased phosphorylation of ULK1 and the reduction of the p62/SQSTM1 protein. However, it also impressed that the expression of transcriptional coactivator peroxisome proliferator-activated receptor gamma coactivator 1 alpha (PGC-1 α) and its downstream target Nrf2 were both significantly increased after the treatment of C3G in HCC94 (Figure 5(a)).

To further investigate the effect of C3G on the mitophagy of HCC94 cells, proteins involved in mitophagy were determined by the Western blot (Figure 5(b)). The results showed that C3G (8 and 20 μM) had a moderate effect on the mitophagy-related genes including ATG5, Parkin, PINK, Beclin1, and VDAC. It seems that C3G did not significantly induce the mitophagy process in HCC94.

Since PGC-1 α expression was elevated with C3G treatment, we wonder whether the combination of C3G and PGC-1 α inhibitor would synergistically affect the treatment

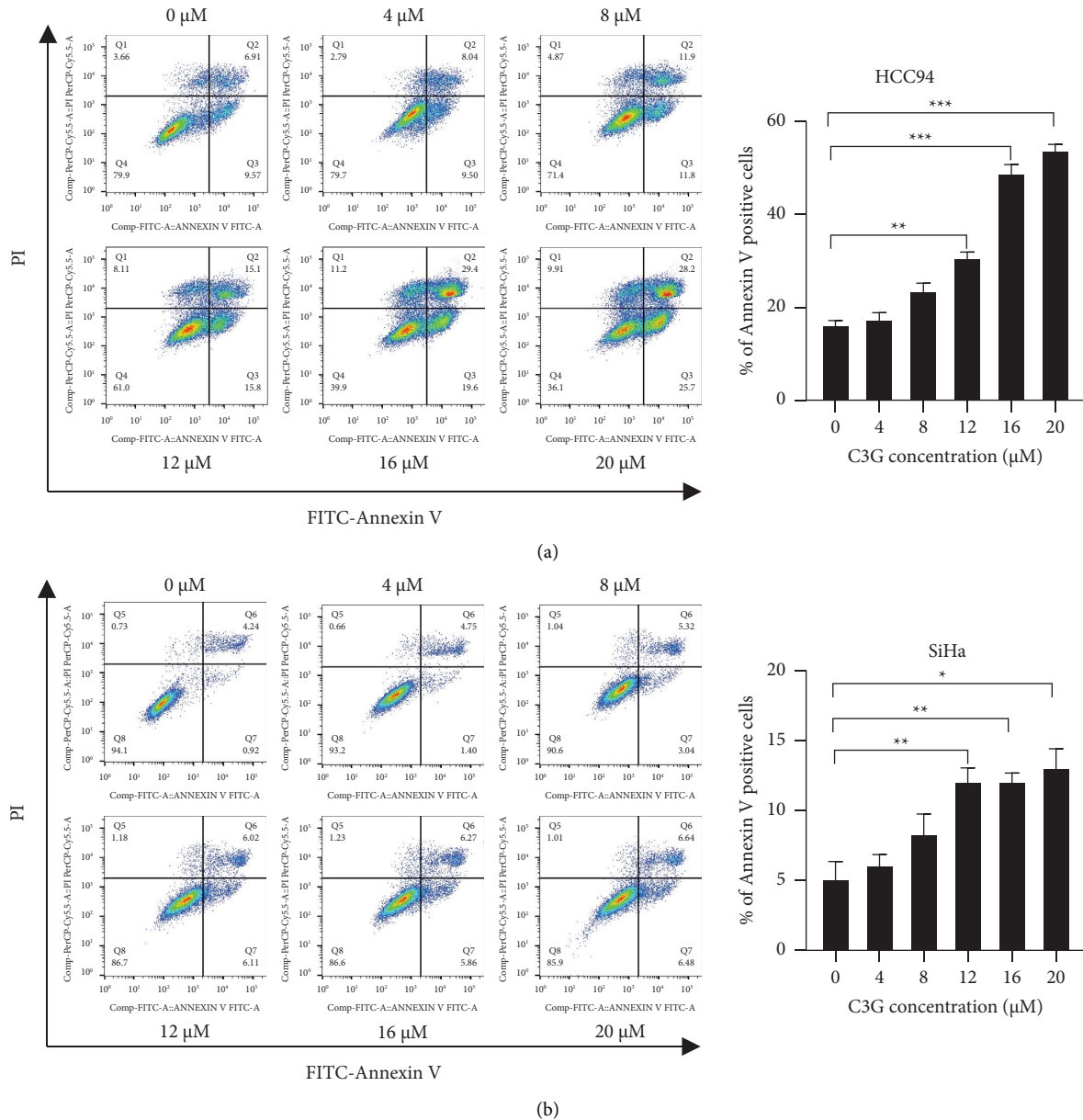


FIGURE 2: (a) The representative images from flow cytometry analysis with Annexin V-PI staining in HCC94 cells treated with different concentrations of C3G were shown in the left panel, and the statistical analysis results were presented in the right panel. (b) The corresponding results in SiHa cells. Data are expressed as the mean \pm S.E.M. * $P < 0.05$, ** $P < 0.01$, and *** $P < 0.001$.

of CSCC. HCC94 cells were treated with C3G (8 μM), NAC (10 μM), PGC-1 α inhibitor SR-18292 (10 μM), and C3G combined with NAC (or SR-18292) for 48 h. The Western blot results showed that C3G combined with SR-18292 would induce autophagy more powerful by decreasing the phosphorylation of ULK1 and increased the cleaved LC-3II compared to the C3G treated alone (Figure 5(c)). More critical, C3G combined with SR-18292 significantly increased the accumulation of intracellular ROS compared to the C3G treated alone (* $P < 0.05$, Figure 5(d)), and the level of ROS decreased in cells treated with C3G plus antioxidant NAC. In addition, the statistical analysis results are shown in Figure S1, and the original raw data of Western blots are provided in Figure S2.

Taken together, our present results suggested that C3G promoted the autophagy process and ROS accumulation, but at the same time, it caused the activation of PGC-1 α mediated mitochondrial biogenesis. The combination of C3G and PGC-1 α inhibitor SR-18292 showed a synergistic effect on the treatment of CSCC.

3.6. The Synergistic Effect of C3G and PGC1 α Inhibitors on Cell Proliferation and Mitochondrial Function. To further determine the synergistic effect of C3G and PGC1 α inhibitors on cell proliferation and mitochondrial function, we performed EdU/Hoechst 33342 staining and mitochondrial membrane potential ($\Delta\psi\text{m}$) in both HCC94 and

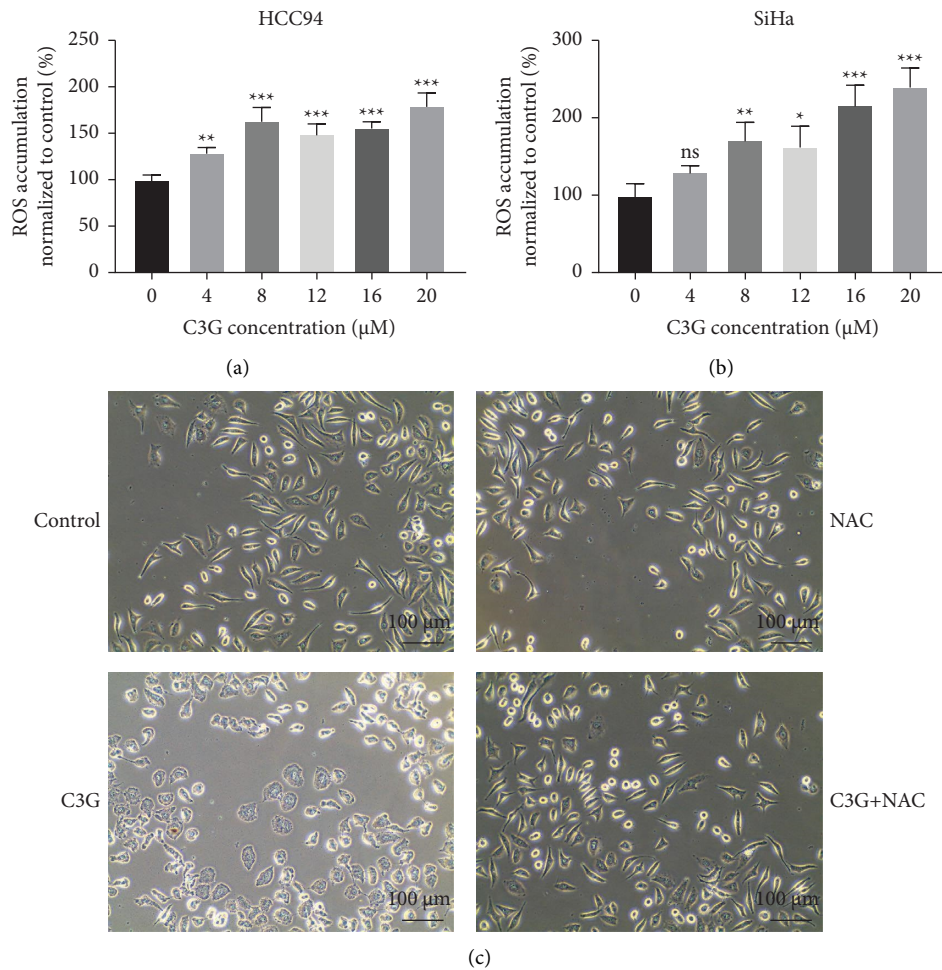


FIGURE 3: Cellular ROS in HCC94 (a) and SiHa (b) cells. The ROS accumulation was expressed as a relative percentage value normalized to control. (c) HCC94 cells were treated with DMSO, NAC (10 μM), C3G (8 μM), and C3G (8 μM) plus NAC (10 μM) for 48 h, respectively. Cell images were obtained after treatment by using a microscope (magnification: 100x). Data are expressed as the mean \pm S.E.M. * $P < 0.05$, ** $P < 0.01$, *** $P < 0.001$, ns: nonsignificant differences. The scale bar is 100 μm .

SiHa cells (Figure 6). Images were obtained and analyzed by Image Pro Plus 6.0, and the statistical result is shown in supplementary materials as Figure S3. The results showed that both Hoechst 33342 and EdU positive cell numbers were decreased after C3G treatment in HCC94 and SiHa cells. More importantly, C3G combined with PGC1 α inhibitors SR-18292 significantly inhibited the proliferation of both HCC94 and SiHa cells compared with C3G treated alone (* $P < 0.05$, Figures 6(a) and S3). However, the antioxidants NAC seem to promote the proliferation of cancer cells.

The effect of C3G combined with PGC1 α inhibitors SR-18292 on mitochondrial function was further determined by the mitochondrial membrane potential ($\Delta\psi\text{m}$) assay (Figure 6(b)). As the same results showed in Figure 4, C3G decreased the JC-1 aggregate. In contrast, the PGC1 α inhibitors SR-18292 weakly affected mitochondrial membrane potential. However, the results indicated that the combination had a more powerful impact on the mitochondrial membrane potential ($\Delta\psi\text{m}$) damage, which would cause mitochondrial dysfunction and cell death.

4. Discussion

As the most widely distributed anthocyanin in fruits and vegetables, cyanidin-3-O-glucoside (C3G) has been reported to possess antioxidant activities and would be a potent therapy strategy for various diseases [39, 40]. However, some previous studies indicated that its antioxidant efficiency is decreased compared with cyanidin due to the existence of a sugar group [26]. In cervical cancer, our present study demonstrated that C3G inhibited the cell growth of CSCC cells, induced cellular ROS accumulation, and destroyed the mitochondrial membrane potential, further promoting the CSCC cells' apoptosis and autophagy. However, some of our results indicated that C3G enhanced the biogenesis of mitochondria simultaneously, such as the elevated expression of the PGC-1 α signaling pathway proteins and the increased mass of mitochondria in cells treated with higher concentrations of C3G. Therefore, we suspected that the decreased efficiency of C3G on cancer cells may be due to the feedback of the biogenesis of mitochondria. When CSCC cells experienced severe damage to mitochondria under the

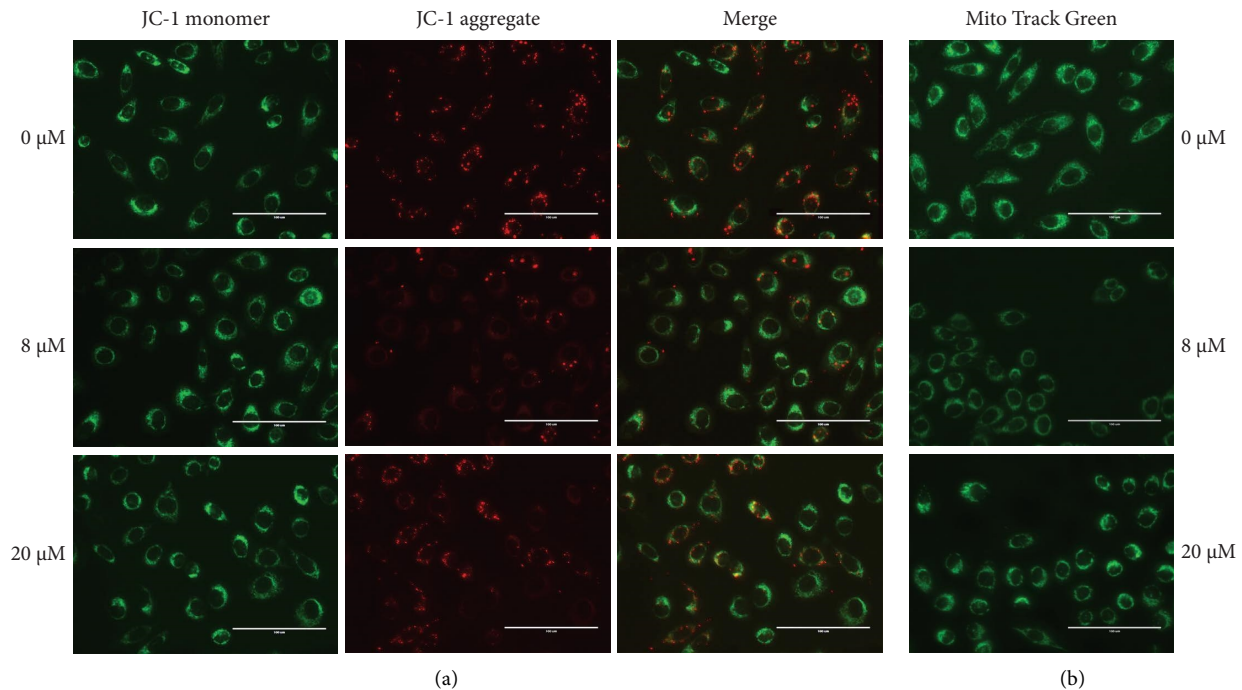


FIGURE 4: (a) Mitochondrial membrane potential assay to detect the effect of C3G (8 and 20 μM) on the $\Delta\psi\text{m}$ reduction of HCC94 cells. Fluorescence images were obtained after 48 h treatment, and representative images of JC-1 monomer (green), JC-1 aggregate (red), and merge were shown. Scale bar: 100 μm . (b) Mito-track green staining to detect the mitochondrial mass of HCC94 treated with C3G (8 and 20 μM) for 48 h. Scale bar: 100 μm .

treatment of C3G, the biogenesis signal was stimulated, and cells tried to repair or remove the mitochondria; this response would rescue cells from damage caused by C3G and finally decrease the efficiency of C3G on cancer. To block the feedback response, we tried to test the synergistic effect of C3G with the PGC1 α inhibitor SR-18292. Our results suggested that C3G combined SR-18292 significantly increased the level of cellular ROS in CSCC cells compared with C3G alone. In addition, the combination of C3G and SR-18292 showed a significant synergistic effect on cell proliferation inhibition and mitochondrial membrane potential damage. Therefore, our present study suggests a new potential therapeutic strategy for CSCC based on the synergistic effect of C3G and PGC1 α inhibitors.

Mitophagy is one form of autophagy and refers to the selective targeting and removal of mitochondria through lysosomal degradation. In some stress conditions such as ROS stimulation, nutrition deficiency, and cell senescence, cells undergo mitophagy to maintain mitochondria homeostasis [41, 42]. However, some reports indicated mitophagy would be suppressed when cells cannot handle many damaged or dysfunctional mitochondria under severe conditions. In our study, the mitophagy-related proteins such as PINK, Parkin, VDAC1, and Beclin had nonobvious

alternation, which indicates the low-intensity activation of mitophagy caused by C3G. These results suggested that C3G promoted the ROS accumulation and dysfunction of mitochondria, which further induced cells to undergo apoptosis and autophagy but not mitophagy mainly.

PGC-1 α expression was significantly increased with C3G treatment, and the possible mechanisms underlying this phenomenon would be due to the severe mitochondrial damage caused by C3G and the feedback activity of the mitochondria biogenesis pathway. PGC-1 α has been characterized as a master regulator of mitochondrial biogenesis and a central player in regulating the antioxidant defense [43]. In addition, PGC-1 α was highly inducible under stressful conditions in cells to maintain mitochondrial homeostasis. PGC-1 α positively increased mitochondrial biogenesis and elevated the cellular ROS-detoxifying capacity, and the loss of PGC-1 α would cause severe mitochondrial dysfunction [44, 45]. In our present results, C3G treatment induced an elevated PGC-1 α and Nrf2 expression in HCC94. Combined with the results of Mito-track green staining, it indicated that C3G may activate the PGC-1 α signaling pathway and increase the biogenesis of mitochondria. We supposed that the enhanced mitochondrial biogenesis would be a feedback

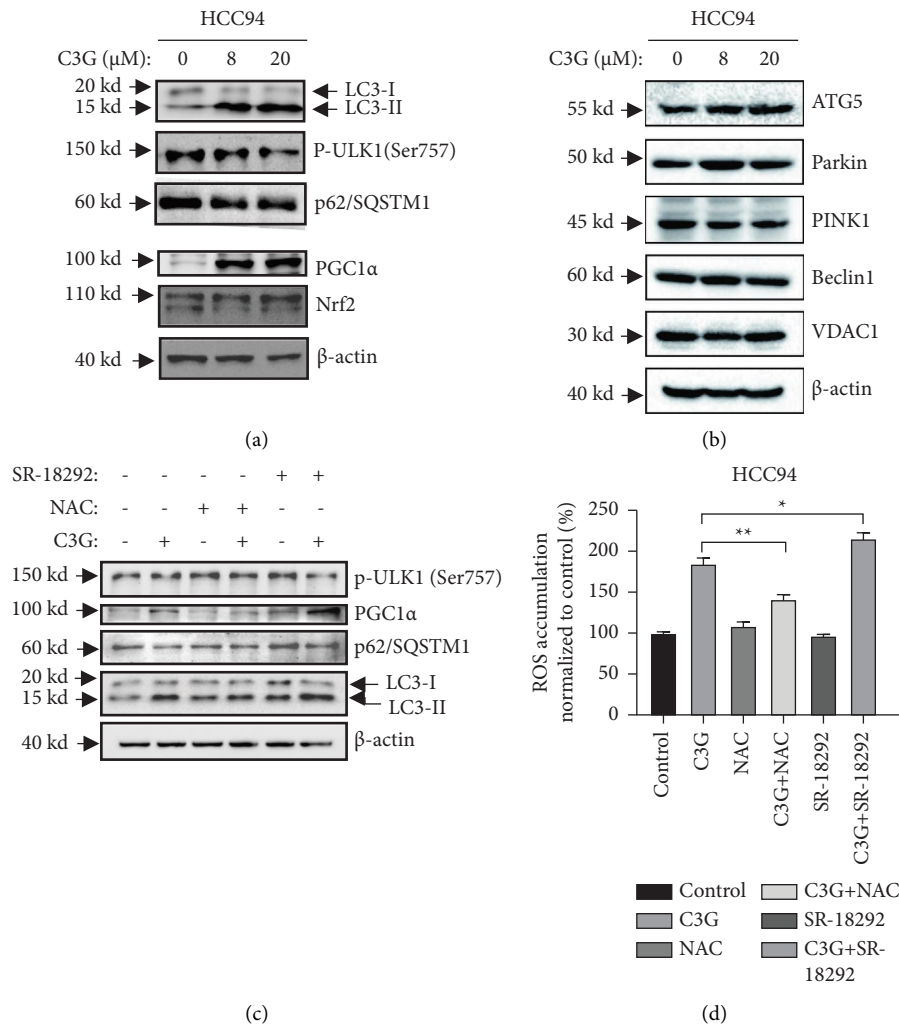


FIGURE 5: (a) The effect of C3G (0, 8, and 20 μM) on autophagy-related proteins. (b) The impact of C3G (0, 8, and 20 μM) on mitophagy-related proteins. (c) The effect of C3G, NAC, SR-18292, and their combination treatment on autophagy-related proteins. (d) The level of ROS in cells treated with C3G (8 μM), NAC (10 μM), SR-18292 (10 μM), and their combination for 48 h. The ROS accumulation was expressed as a relative percentage value normalized to control. Data are expressed as the mean \pm S.E.M. * $P < 0.05$ and ** $P < 0.01$.

response to the predominantly mitochondrial damage caused by C3G-induced ROS accumulation, which finally decreases the therapeutic efficiency of C3G on CSCC cells. In addition, there are some limits to this study. The effect of

C3G combined with PGC1 α inhibitors on CSCC cells must be further tested both *in vitro* and *in vivo*. We proposed a novel therapeutic strategy for CSCC based on the synergistic effect of C3G and PGC1 α inhibitors.

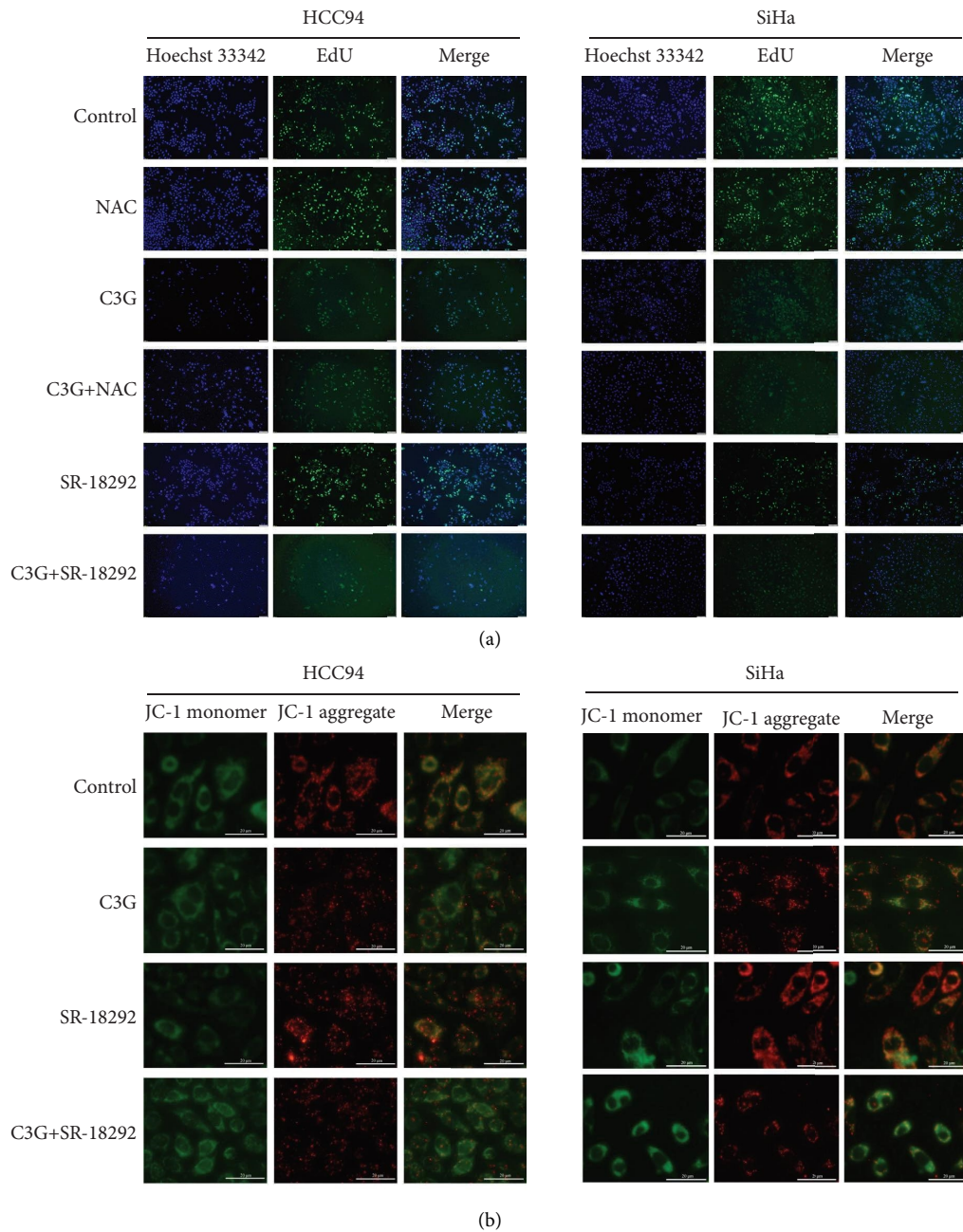


FIGURE 6: (a) The effect of C3G ($8 \mu\text{M}$), NAC ($10 \mu\text{M}$), SR-18292 ($10 \mu\text{M}$), and their combination treatment on cell proliferation was determined by EdU/Hoechst 33342 staining. Scale bar: $50 \mu\text{m}$. (b) Mitochondrial membrane potential assay to detect the effect of C3G alone ($8 \mu\text{M}$), SR-18292 alone ($10 \mu\text{M}$), and the combination of C3G ($8 \mu\text{M}$) and SR-18292 ($10 \mu\text{M}$) on the $\Delta\psi\text{m}$ reduction of HCC94 and SiHa cells. Fluorescence images were obtained after 48 h treatment, and representative images of JC-1 monomer (green), JC-1 aggregate (red), and merge were shown. Scale bar: $20 \mu\text{m}$.

Data Availability

The original Western blot data used to support the findings of this study are available from the corresponding author upon request.

Conflicts of Interest

The authors declare that they have no conflicts of interest.

Authors' Contributions

Lili Liu performed investigation and writing of the original draft; Tao Zhao conducted investigation; Huaping Yang carried out investigation; Zhenghui Hu performed investigation; Caifeng Xie conducted supervision, funding acquisition, writing, review, and editing. All authors have read and agreed to the published version of the manuscript. Lili Liu and Tao Zhao contributed equally to this work.

Acknowledgments

This study was partially supported by grants from the National Natural Science Foundation of China (82260563), Jiangxi Provincial Natural Science Foundation (20232BAB206105), and the Training Program for Academic and Technical Young Leaders of Major Disciplines in Jiangxi Province (20232BCJ23042).

Supplementary Materials

Supplementary 1. Table S1. The list of antibodies used in this paper. Supplementary 2. Figure S1. The quantification results of Western blot bands in Figure 5. Supplementary 3. Figure S2. The original images of Western blot bands in Figure 5. Supplementary 4. Figure S3. The quantification results of the EdU/Hoechst 33342 staining assay in Figure 6. (*Supplementary Materials*)

References

- [1] H. Sung, J. Ferlay, R. L. Siegel et al., "Global cancer statistics 2020: GLOBOCAN estimates of incidence and mortality worldwide for 36 cancers in 185 countries," *CA: A Cancer Journal for Clinicians*, vol. 71, no. 3, pp. 209–249, 2021.
- [2] P. A. Cohen, A. Jhingran, A. Oaknin, and L. Denny, "Cervical cancer," *The Lancet*, vol. 393, no. 10167, pp. 169–182, 2019.
- [3] M. Mann, V. P. Singh, and L. Kumar, "Cervical cancer: a tale from HPV infection to PARP inhibitors," *Genes and Diseases*, vol. 10, no. 4, pp. 1445–1456, 2023.
- [4] C. A. Burmeister, S. F. Khan, G. Schäfer et al., "Cervical cancer therapies: current challenges and future perspectives," *Tumour Virus Research*, vol. 13, Article ID 200238, 2022.
- [5] S. Kaur, L. M. Sharma, V. Mishra et al., "Challenges in cervical cancer prevention: real-world scenario in India," *South Asian Journal of Cancer*, vol. 12, no. 01, pp. 009–016, 2023.
- [6] S. H. Park, M. Kim, S. Lee, W. Jung, and B. Kim, "Therapeutic potential of natural products in treatment of cervical cancer: a review," *Nutrients*, vol. 13, no. 1, p. 154, 2021.
- [7] Z. W. Zhou, H. Z. Long, S. G. Xu et al., "Therapeutic effects of natural products on cervical cancer: based on inflammatory pathways," *Frontiers in Pharmacology*, vol. 13, Article ID 899208, 2022.
- [8] M. A. Esmaeili, N. Abagheri-Mahabadi, H. Hashempour, M. Farhadpour, C. W. Gruber, and A. Ghassempour, "Viola plant cyclotide vigno 5 induces mitochondria-mediated apoptosis via cytochrome C release and caspases activation in cervical cancer cells," *Fitoterapia*, vol. 109, pp. 162–168, 2016.
- [9] E. C. Cheung and K. H. Vousden, "The role of ROS in tumour development and progression," *Nature Reviews Cancer*, vol. 22, no. 5, pp. 280–297, 2022.
- [10] B. Perillo, M. Di Donato, A. Pezone et al., "ROS in cancer therapy: the bright side of the moon," *Experimental and Molecular Medicine*, vol. 52, no. 2, pp. 192–203, 2020.
- [11] M. A. Shah and H. A. Rogoff, "Implications of reactive oxygen species on cancer formation and its treatment," *Seminars in Oncology*, vol. 48, no. 3, pp. 238–245, 2021.
- [12] D. Trachootham, J. Alexandre, and P. Huang, "Targeting cancer cells by ROS-mediated mechanisms: a radical therapeutic approach?" *Nature Reviews Drug Discovery*, vol. 8, no. 7, pp. 579–591, 2009.
- [13] S. J. Kim, H. S. Kim, and Y. R. Seo, "Understanding of ROS-inducing strategy in anticancer therapy," *Oxidative Medicine and Cellular Longevity*, vol. 2019, Article ID 5381692, 12 pages, 2019.
- [14] Y. Chen, Y. Li, L. Huang et al., "Antioxidative stress: inhibiting reactive oxygen species production as a cause of radioresistance and chemoresistance," *Oxidative Medicine and Cellular Longevity*, vol. 2021, Article ID 6620306, 16 pages, 2021.
- [15] O. Abu Shelbayeh, T. Arroum, S. Morris, and K. B. Busch, "PGC-1 α is a master regulator of mitochondrial lifecycle and ROS stress response," *Antioxidants*, vol. 12, no. 5, p. 1075, 2023.
- [16] J. St-Pierre, S. Drori, M. Uldry et al., "Suppression of reactive oxygen species and neurodegeneration by the PGC-1 transcriptional coactivators," *Cell*, vol. 127, no. 2, pp. 397–408, 2006.
- [17] W. Zheng and S. Y. Wang, "Oxygen radical absorbing capacity of phenolics in blueberries, cranberries, chokeberries, and lingonberries," *Journal of Agricultural and Food Chemistry*, vol. 51, no. 2, pp. 502–509, 2003.
- [18] M. Ding, R. Feng, S. Y. Wang et al., "Cyanidin-3-glucoside, a natural product derived from blackberry, exhibits chemopreventive and chemotherapeutic activity," *Journal of Biological Chemistry*, vol. 281, no. 25, pp. 17359–17368, 2006.
- [19] M. Xu, K. A. Bower, S. Wang et al., "Cyanidin-3-glucoside inhibits ethanol-induced invasion of breast cancer cells overexpressing ErbB2," *Molecular Cancer*, vol. 9, no. 1, p. 285, 2010.
- [20] P. N. Chen, S. C. Chu, H. L. Chiou, C. L. Chiang, S. F. Yang, and Y. S. Hsieh, "Cyanidin 3-glucoside and peonidin 3-glucoside inhibit tumor cell growth and induce apoptosis in vitro and suppress tumor growth in vivo," *Nutrition and Cancer*, vol. 53, no. 2, pp. 232–243, 2005.
- [21] Y. Zhou, L. Chen, D. Ding et al., "Cyanidin-3-O-glucoside inhibits the β -catenin/MGMT pathway by upregulating miR-214-5p to reverse chemotherapy resistance in glioma cells," *Scientific Reports*, vol. 12, no. 1, p. 7773, 2022.
- [22] V. Sorrenti, L. Vanella, R. Acquaviva, V. Cardile, S. Giorfrè, and C. Di Giacomo, "Cyanidin induces apoptosis and differentiation in prostate cancer cells," *International Journal of Oncology*, vol. 47, no. 4, pp. 1303–1310, 2015.
- [23] Y. Jia, C. Wu, A. Rivera-Piza, Y. J. Kim, J. H. Lee, and S. J. Lee, "Mechanism of action of cyanidin 3-O-glucoside in

- gluconeogenesis and oxidative stress-induced cancer cell senescence,” *Antioxidants*, vol. 11, no. 4, p. 749, 2022.
- [24] X. Li, J. Mu, Y. Lin, J. Zhao, and X. Meng, “Combination of cyanidin-3-O-glucoside and cisplatin induces oxidative stress and apoptosis in HeLa cells by reducing activity of endogenous antioxidants, increasing bax/bcl-2 mRNA expression ratio, and downregulating Nrf2 expression,” *Journal of Food Biochemistry*, vol. 45, no. 7, Article ID e13806, 2021.
- [25] W. Sun, N. D. Zhang, T. Zhang et al., “Cyanidin-3-O-Glucoside induces the apoptosis of human gastric cancer MKN-45 cells through ROS-mediated signaling pathways,” *Molecules*, vol. 28, no. 2, p. 652, 2023.
- [26] M. Takeuchi, K. Ohtani, Y. Ma et al., “Differential effects of cyanidin and cyanidin-3-glucoside on human cell lines,” *Food Science and Technology Research*, vol. 17, no. 6, pp. 515–521, 2011.
- [27] X. Li, J. Zhao, T. Yan et al., “Cyanidin-3-O-glucoside and cisplatin inhibit proliferation and downregulate the PI3K/AKT/mTOR pathway in cervical cancer cells,” *Journal of Food Science*, vol. 86, no. 6, pp. 2700–2712, 2021.
- [28] J. Jin, Z. Zhang, S. Zhang et al., “Fatty acid binding protein 4 promotes epithelial-mesenchymal transition in cervical squamous cell carcinoma through AKT/GSK3 β /Snail signaling pathway,” *Molecular and Cellular Endocrinology*, vol. 461, pp. 155–164, 2018.
- [29] X. Zhao, Y. Zhang, and Y. Su, “Establishment and characterization of a xenografted human cervical carcinoma in nude mice and homologous cell line in vitro,” *Zhonghua Fu Chan Ke Za Zhi*, vol. 32, no. 4, pp. 217–221, 1997.
- [30] Z. Lu, T. Han, T. Wang et al., “OXCT1 regulates NF- κ B signaling pathway through β -hydroxybutyrate-mediated ketone body homeostasis in lung cancer,” *Genes and Diseases*, vol. 10, no. 2, pp. 352–355, 2023.
- [31] H. U. Simon, A. Haj-Yehia, and F. Levi-Schaffer, “Role of reactive oxygen species (ROS) in apoptosis induction,” *Apoptosis*, vol. 5, no. 5, pp. 415–418, 2000.
- [32] A. Eckert, U. Keil, C. A. Marques et al., “Mitochondrial dysfunction, apoptotic cell death, and Alzheimer’s disease,” *Biochemical Pharmacology*, vol. 66, no. 8, pp. 1627–1634, 2003.
- [33] Y. Luo, J. Ma, and W. Lu, “The significance of mitochondrial dysfunction in cancer,” *International Journal of Molecular Sciences*, vol. 21, no. 16, p. 5598, 2020.
- [34] L. D. Zorova, V. A. Popkov, E. Y. Plotnikov et al., “Mitochondrial membrane potential,” *Analytical Biochemistry*, vol. 552, pp. 50–59, 2018.
- [35] S. Liu, S. Liu, B. He et al., “OXPHOS deficiency activates global adaptation pathways to maintain mitochondrial membrane potential,” *EMBO Reports*, vol. 22, no. 4, Article ID e51606, 2021.
- [36] M. Onishi, K. Yamano, M. Sato, N. Matsuda, and K. Okamoto, “Molecular mechanisms and physiological functions of mitophagy,” *The EMBO Journal*, vol. 40, no. 3, Article ID e104705, 2021.
- [37] F. Randow and R. J. Youle, “Self and nonself: how autophagy targets mitochondria and bacteria,” *Cell Host and Microbe*, vol. 15, no. 4, pp. 403–411, 2014.
- [38] I. Tanida, T. Ueno, and E. Kominami, “LC3 and autophagy,” *Methods in Molecular Biology*, vol. 445, pp. 77–88, 2008.
- [39] M. S. Molonia, C. Occhiuto, C. Muscarà et al., “Cyanidin-3-O-glucoside restores insulin signaling and reduces inflammation in hypertrophic adipocytes,” *Archives of Biochemistry and Biophysics*, vol. 691, Article ID 108488, 2020.
- [40] F. J. Olivás-Aguirre, J. Rodrigo-García, N. D. Martínez-Ruiz et al., “Cyanidin-3-O-glucoside: physical-chemistry, foodomics and health effects,” *Molecules*, vol. 21, no. 9, p. 1264, 2016.
- [41] J. J. Lemasters, “Selective mitochondrial autophagy, or mitophagy, as a targeted defense against oxidative stress, mitochondrial dysfunction, and aging,” *Rejuvenation Research*, vol. 8, no. 1, pp. 3–5, 2005.
- [42] S. A. Killackey, D. J. Philpott, and S. E. Girardin, “Mitophagy pathways in health and disease,” *Journal of Cell Biology*, vol. 219, no. 11, Article ID e202004029, 2020.
- [43] J. F. Halling and H. Pilegaard, “PGC-1 α -mediated regulation of mitochondrial function and physiological implications,” *Applied Physiology Nutrition and Metabolism*, vol. 45, no. 9, pp. 927–936, 2020.
- [44] S. Austin and J. St-Pierre, “PGC1 α and mitochondrial metabolism--emerging concepts and relevance in ageing and neurodegenerative disorders,” *Journal of Cell Science*, vol. 125, no. 21, pp. 4963–4971, 2012.
- [45] L. Chen, Y. Qin, B. Liu et al., “PGC-1 α -Mediated mitochondrial quality control: molecular mechanisms and implications for heart failure,” *Frontiers in Cell and Developmental Biology*, vol. 10, Article ID 871357, 2022.